

# Rotational Symmetry Field Design on Surfaces

Jonathan Palacios\*  
Oregon State University

Eugene Zhang\*  
Oregon State University

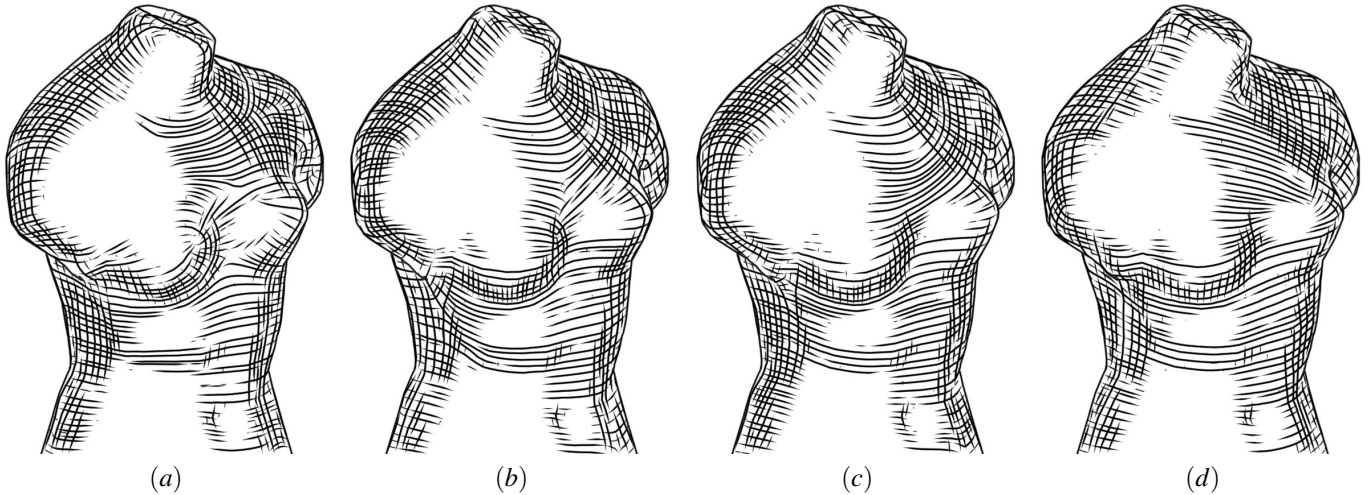


Figure 1: Pen-and-ink sketching of the Venus using four different fields: (a) the curvature tensor smoothed as a 2-RoS field, (b) the curvature tensor smoothed as a 4-RoS field, (c) topological editing operations applied to (b), and (d) more global smoothing performed on (b). Notice that treating the curvature tensor as a 4-RoS field (b) leads to fewer unnatural singularities and therefore less visual artifacts than as a 2-RoS field (a). In addition, both topological editing (c) and global smoothing (d) can be used to remove more singularities from (b). However, topological editing (c) provides local control while excessive global smoothing (d) can cause hatch directions to deviate from their natural orientations (neck and chest).

## Abstract

Designing rotational symmetries on surfaces is a necessary task for a wide variety of graphics applications, such as surface parameterization and remeshing, painterly rendering and pen-and-ink sketching, and texture synthesis. In these applications, the *topology* of a rotational symmetry field such as *singularities* and *separatrices* can have a direct impact on the quality of the results. In this paper, we present a design system that provides control over the topology of rotational symmetry fields on surfaces.

As the foundation of our system, we provide comprehensive analysis for rotational symmetry fields on surfaces and present efficient algorithms to identify singularities and separatrices. We also describe design operations that allow a rotational symmetry field to be created and modified in an intuitive fashion by using the idea of basis fields and relaxation. In particular, we provide control over the topology of a rotational symmetry field by allowing the user to remove singularities from the field or to move them to more desirable locations.

\*e-mail: {palacijo|zhang}@eecs.oregonstate.edu

### ACM Reference Format

Palacios, J., Zhang, E. 2007. Rotational Symmetry Field Design on Surfaces. *ACM Trans. Graph.* 26, 3, Article 55 (July 2007), 10 pages. DOI = 10.1145/1239451.1239506 <http://doi.acm.org/10.1145/1239451.1239506>

### Copyright Notice

Permission to make digital or hard copies of part or all of this work for personal or classroom use is granted without fee provided that copies are not made or distributed for profit or direct commercial advantage and that copies show this notice on the first page or initial screen of a display along with the full citation. Copyrights for components of this work owned by others than ACM must be honored. Abstracting with credit is permitted. To copy otherwise, to republish, to post on servers, to redistribute to lists, or to use any component of this work in other works requires prior specific permission and/or a fee. Permissions may be requested from Publications Dept., ACM, Inc., 2 Penn Plaza, Suite 701, New York, NY 10121-0701, fax +1 (212) 869-0481, or [permissions@acm.org](mailto:permissions@acm.org).  
© 2007 ACM 0730-0301/2007/03-ART55 \$5.00 DOI 10.1145/1239451.1239506  
<http://doi.acm.org/10.1145/1239451.1239506>

At the core of our analysis and design implementations is the observation that  $N$ -way rotational symmetries can be described by symmetric  $N$ -th order tensors, which allows an efficient vector-based representation that not only supports coherent definitions of arithmetic operations on rotational symmetries but also enables many analysis and design operations for vector fields to be adapted to rotational symmetry fields.

To demonstrate the effectiveness of our approach, we apply our design system to pen-and-ink sketching and geometry remeshing.

**CR Categories:** I.3.5 [Computer Graphics]: Computational Geometry and Object Modeling—Geometric algorithms, languages, and systems;

**Keywords:** rotational symmetry, field design, field analysis, surfaces, topology, non-photorealistic rendering, remeshing.

## 1 Introduction

Many objects in computer graphics can be described by *rotational symmetries*, such as brush strokes and hatches in non-photorealistic rendering, regular patterns in texture synthesis, and principle curvature directions in surface parameterization and geometry remeshing. Intuitively, an  $N$ -way rotational symmetry ( $N$ -RoSy) represents phenomena that are *invariant* under rotations of an integer multiple of  $\frac{2\pi}{N}$ . Example  $N$ -RoSy's include a vector ( $N = 1$ ), an eigenvector of a symmetric matrix ( $N = 2$ ), and a cross ( $N = 4$ ).

Symmetries naturally appear in surfaces, such as the five Platonic shapes (Figure 2). Notice that the order of the symmetry  $N$  is equal to the ratio between  $2\pi$  and the angle of deficit at a vertex. In sur-

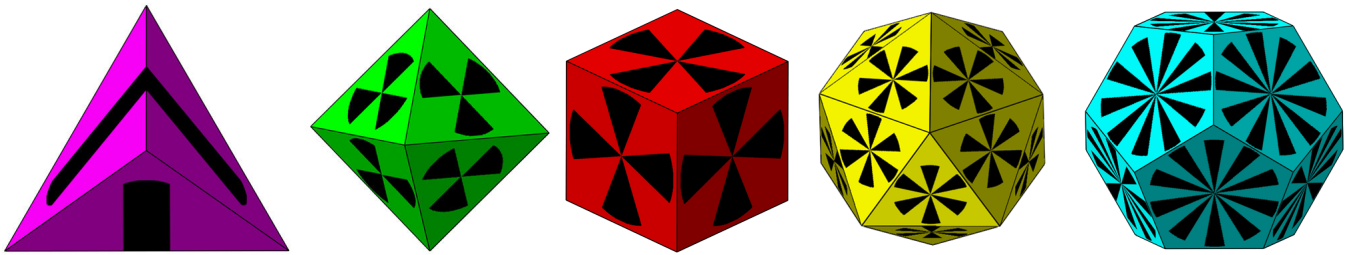


Figure 2:  $N$ -way rotational symmetries appear naturally in the Platonic solids: tetrahedron ( $N = 2$ ), octahedron ( $N = 3$ ), cube ( $N = 4$ ), icosahedron ( $N = 6$ ), and dodecahedron ( $N = 10$ ).

faces where global symmetry is lacking, local symmetries can still occur, such as the singularities (the vertices). In Figure 1 (c), singularities of a 4-RoSy field appear in natural places such as the corner of the shoulder (not visible due to the highlight) and under the armpit.

The ability to design and control  $N$ -RoSy fields on surfaces is essential in many applications. For example, in non-photorealistic rendering, the orientation of brush strokes and hatches are usually guided by an  $N$ -RoSy field. Different artistic effects can be achieved by using guiding fields with different characteristics. In addition, singularities in the guiding field can lead to visual artifacts such as brush strokes and hatches with unnatural orientations. Singularities also present difficulties in the construction of a global surface parameterization, where a significant amount of stretch can occur in nearby regions. Similarly, it is difficult to produce ideal triangular and quad elements near singularities in geometry remeshing. For these applications, a design system can be used to create a wide variety of  $N$ -RoSy fields on surfaces, to add desirable features in an existing field, and to control the number and location of the singularities in the field. Most existing design systems focus on vectors ( $N = 1$ ) [Praun et al. 2000; Turk 2001; Wei and Levoy 2001; Theisel 2002; Stam 2003; Zhang et al. 2006] and tensors ( $N = 2$ ) [Zhang et al. 2007]. A number of difficulties must be addressed before a general design system can be developed for  $N \geq 3$ .

First, there has been a lack of a mathematical representation for rotational symmetries, which is required to define algebraic operations on  $N$ -RoSy's such as sums and scalar multiples as well as important concepts of  $N$ -RoSy fields such as singularities, continuity, and differentiability. We overcome this difficulty by embedding  $N$ -way rotational symmetries in the space of  $N$ -th order tensors, which allows algebraic operations to be carried over from  $N$ -th order tensors to  $N$ -RoSy's. We further derive a vector-based representation of rotational symmetries based on the embedding, which enables efficient analysis of  $N$ -RoSy fields on surfaces as well as allows vector field design functionalities to be adapted to  $N$ -RoSy fields. Furthermore, the concepts of singularities, continuity, and differentiability are well-defined.

Second, there is relatively little understanding of the topological structure in an  $N$ -RoSy field. While the concepts of singularities have been used before, a proper definition of separatrices is missing when  $N \geq 3$ . To address this, we present efficient algorithms on extracting the singularities and separatrices in a field. In particular, we adopt the approach of Zhang et al. [2006] that allows continuous  $N$ -RoSy fields to be generated on mesh surfaces despite the discontinuity in the surface normal.

With the above issues addressed, we present a design system for  $N$ -RoSy fields on surfaces that not only allows a wide variety of  $N$ -RoSy fields to be generated but also provides explicit control over the number and location of the singularities in the field. The main

functionalities of our work is reminiscent of that for vector field design [Zhang et al. 2006]. However, the implementations are rather different. For instance, we can create an initial  $N$ -RoSy field on a surface using relaxation techniques [Turk 2001] which do not require a global surface parameterization. This greatly increases the interactivity of our system. We also reuse algorithms for singularity pair cancellation and movement in vector fields through the aforementioned vector-based representation.

We have applied our design system to graphics applications such as pen-and-ink sketching and quad-dominant remeshing.

In this paper, we make the following contributions.

1. We provide coherent definitions for algebraic operations on  $N$ -RoSy's by observing the link between  $N$ -RoSy's and  $N$ -th order symmetric tensors. This link also enables the definitions of analytic properties of  $N$ -RoSy fields such as continuity, differentiability, and singularity.
2. We present a vector-based representation for  $N$ -RoSy's that supports compact storage of discrete  $N$ -RoSy fields on mesh surfaces and facilitates the analysis and design of  $N$ -RoSy fields.
3. We describe the topology of  $N$ -RoSy fields on surfaces and provide efficient algorithms to extract singularities and separatrices.
4. We develop a design system in which  $N$ -RoSy fields can be interactively created and modified on surfaces. In particular, our system provides explicit control over the number and location of the singularities in the field. We demonstrate the effectiveness of our system with pen-and-ink sketching of surfaces and quad-dominant remeshing.

The remainder of the paper is organized as follows. We first review related work on  $N$ -RoSy fields in Section 2 and present our vector-based representation of  $N$ -RoSy's in Section 3. Next, we discuss the analysis and design of  $N$ -RoSy fields in Sections 4 and 5, respectively. In Section 6, we show the results of applying our analysis and design system to pen-and-ink sketching and geometry remeshing. Finally, we summarize our contributions and discuss some possible future work in Section 7.

## 2 Previous Work

There has been a significant amount of work in the analysis and design of vector and tensor fields. In contrast, relatively little is known about  $N$ -RoSy fields when  $N \geq 3$ .

**$N$ -RoSy Analysis and Design:** To the best of our knowledge, Hertzmann and Zorin [2000] are the first to propose that hatches should follow a cross field (4-RoSy). They provide a smoothing

operation on 4-RoSy fields that is based on a non-linear optimization. Ray et al. [2006a] construct a periodic global parameterization that facilitates quad remeshing. At the heart of their approach is the use of 4-RoSy fields, which allows more natural-shaped quads to be generated near singularities. They also develop a framework that allows the optimization to be performed on the sines and cosines of the parameterization, which turns a non-linear optimization into a linear one. They later provide the analysis of singularities on  $N$ -RoSy's by extending the Poincaré-Hopf theorem as well as describe an algorithm in which a field with a minimal number of singularities can be constructed based on user-specified constraints and the Euler characteristic of the underlying surface [Ray et al. 2006b].

**Vector and Tensor Field Design:** There have been a number of vector field design systems for surfaces. Most of them are generated for a particular graphics application such as texture synthesis [Praun et al. 2000; Turk 2001; Wei and Levoy 2001], fluid simulation [Stam 2003], and vector field visualization [van Wijk 2002; van Wijk 2003]. These systems do not address topological control in the field. Systems providing topological control include [Theisel 2002; Zhang et al. 2006]. The system of Zhang et al. has also been extended to create periodic orbits [Chen et al. 2007] and to design tensor fields [Zhang et al. 2007]. Our system is also reminiscent of the vector field design system of Zhang et al. [2006] in terms of the functionality. However, the implementation is rather different.

**Vector and Tensor Field Analysis:** There has been much work in vector and tensor field analysis. To review all the work is beyond the scope of this paper. Here we refer to the most relevant work. Helman and Hesselink [1991] propose vector field visualization techniques based on topological analysis. Delmarcelle and Hesselink provide analysis of second-order symmetric tensor fields [1994].

### 3 Vector-Based Representation

The analysis and design of  $N$ -RoSy fields require coherent definitions of the following concepts: summation and scalar multiplication of  $N$ -RoSy's as well as continuity, singularity, and differentiability. However, it is not immediately clear how to define these concepts in a consistent manner given that a non-zero  $N$ -RoSy  $s$  consists of  $N$  directions. For convenience, we will refer to these directions the *member vectors* of  $s$ . Consider the case when  $N = 2$ , i.e., lines that can be modeled by eigenvectors of a symmetric matrix with a zero trace [Zhang et al. 2007]. Given two 2-RoSy's  $s_1 = \{\pm \begin{pmatrix} 1 \\ 0 \end{pmatrix}\}$  and  $s_2 = \{\pm \begin{pmatrix} 0 \\ 1 \end{pmatrix}\}$ , defining  $s_1 + s_2$  as the sum of

member vectors can lead to inconsistent results: (1)  $\{\pm \begin{pmatrix} 1 \\ 1 \end{pmatrix}\}$ , or (2)  $\{\pm \begin{pmatrix} 1 \\ -1 \end{pmatrix}\}$ . As demonstrated by Zhang et al. [2007], treating a line field as a vector field results in discontinuities and inconsistencies. This is also true for  $N$ -RoSy fields when  $N \geq 3$ .

To overcome this problem, we describe a representation for  $N$ -RoSy's that is free of directional ambiguity. For an  $N$ -RoSy

$$s = \left\{ \begin{pmatrix} R \cos(\theta + \frac{2k\pi}{N}) \\ R \sin(\theta + \frac{2k\pi}{N}) \end{pmatrix} \mid 0 \leq k \leq N-1 \right\} \quad (1)$$

where  $R \geq 0$  is the strength of  $s$  and  $\theta$  is the angular component of one of the member vectors, we define the *representation vector* of  $s$  as  $\begin{pmatrix} R \cos N\theta \\ R \sin N\theta \end{pmatrix}$ . Notice that the representation vector is independent of the choice of member vectors since

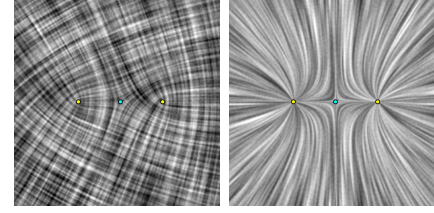


Figure 3: A comparison between a 4-RoSy field (left) and its representation vector field (right). Notice that the sets of points with a zero value are the same for both fields (colored dots). Representation vectors remove the directional ambiguity in an  $N$ -RoSy field.

$$N(\theta + \frac{2k\pi}{N}) \equiv N\theta \pmod{2\pi} \quad (2)$$

for any integer  $k$ . Consequently, directional ambiguity no longer exists under this representation. We will define a map  $\gamma$  which maps an  $N$ -RoSy  $s$  to its representation vector  $\gamma(s)$ . Given two  $N$ -RoSy's  $s_1$  and  $s_2$  and a real number  $\lambda$ , we define

$$s_1 + s_2 = \gamma^{-1}(\gamma(s_1) + \gamma(s_2)), \quad \lambda s_1 = \gamma^{-1}(\lambda \gamma(s_1)) \quad (3)$$

These definitions are coherent as they do not rely on the choice of member vectors, which allow us to define important concepts on  $N$ -RoSy fields, such as continuity, singularity, and differentiability in a consistent manner.

A representation vector and a member vector differ in how their components change under a change of basis. Consider the case where the transformation matrix from the new basis to the original basis has the form  $Q = \begin{pmatrix} \cos \varphi & -\sin \varphi \\ \sin \varphi & \cos \varphi \end{pmatrix}$ . While a member vector  $v$  will have the form  $Qv$  under the new basis, a representation vector  $w$  will be of the form  $Q'w$  where  $Q' = \begin{pmatrix} \cos N\varphi & -\sin N\varphi \\ \sin N\varphi & \cos N\varphi \end{pmatrix}$ . Therefore, a representation vector is not a vector since its components do not change like a vector under changes of basis. In the Appendix, we show that  $N$ -RoSy's can be represented by symmetric  $N$ -th order covariant tensors of a special form and such tensors can be compactly represented by a vector (representation vector) under any given basis. Consequently, the components of a representation vector transform differently than a vector under a change of basis.

As will become apparent soon,  $\gamma$  not only provides a coherent and compact representation of  $N$ -RoSy's, but also allows efficient implementations of key operations on  $N$ -RoSy fields by borrowing corresponding algorithms for vector fields, such as interpolations and singularity extraction (Section 4.3), blending (Section 5.1), and topological editing (Section 5.2). Figure 3 shows a 4-RoSy field (left) and its representation vector field (right). Notice that they have the same set of singularities. Next, we discuss the analysis and design of  $N$ -RoSy fields on surfaces.

### 4 Topological Analysis of $N$ -RoSy Fields

In this section, we describe important topological properties of  $N$ -RoSy fields on manifold surfaces, such as *singularities* and *separatrices*. We will also present efficient algorithms to compute these quantities on mesh surfaces.

Singularity identification is necessary for providing explicit control over the number and location of singularities, which is needed

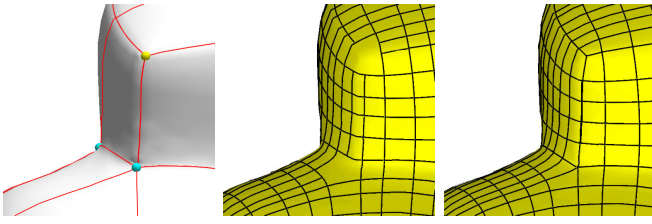


Figure 4: This figure illustrates the importance of singularity and separatrix extraction in quad-dominant remeshing. Given a 3D model (left), the singularities and separatrices are highlighted by colored dots and curves, respectively. Including separatrices during remeshing can lead to better meshes near the singularities (right) than not including them (middle).

in pen-and-ink sketching of 3D surfaces as undesirable singularities cause visual artifacts [Hertzmann and Zorin 2000] (Figures 1 and 7). Singularity and separatrix extraction allow better meshing near singularities during the remeshing process (Section 6.2). Figure 4 illustrates this with a 3D surface obtained by joining two cubes with rounded corners. In the left, the singularities are highlighted by colored dots and the separatrices are the colored curves emanating from the singularities. Notice that singularities appear in natural places (corners and joints) and separatrices indicate important directions near the singularities. Utilizing separatrices during the remeshing process produces meshes that can better maintain features in the original mesh (Figure 4, right) than disregarding them (Figure 4, middle).

The concepts of singularities and separatrices are well defined for vector and tensor fields, i.e., when  $N = 1, 2$ . Next, we will extend them to  $N$ -Rosy fields when  $N \geq 3$ .

#### 4.1 Singularities

For simplicity, consider a planar vector field  $V(x, y) = \begin{pmatrix} F(x, y) \\ G(x, y) \end{pmatrix}$ .

A *singularity*  $\mathbf{p}_0$  is a point in the domain where  $V(\mathbf{p}_0) = 0$ .  $\mathbf{p}_0$  is *isolated* if there exists an open neighborhood  $U$  of  $\mathbf{p}_0$  with the property that  $\mathbf{p}_0$  is the unique singularity in the interior of  $U$  and there are no singularities on the boundary of  $U$ . An isolated singularity  $\mathbf{p}_0$  can be characterized by its *Jacobian*  $DV(\mathbf{p}_0) = \begin{pmatrix} a & b \\ c & d \end{pmatrix}$ , where  $a = \frac{\partial F}{\partial x}(\mathbf{p}_0)$ ,  $b = \frac{\partial F}{\partial y}(\mathbf{p}_0)$ ,  $c = \frac{\partial G}{\partial x}(\mathbf{p}_0)$ , and  $d = \frac{\partial G}{\partial y}(\mathbf{p}_0)$ . The *local linearization* of  $V$  at a point  $\mathbf{p}_0$  is a function  $LV(\mathbf{p}) = DV(\mathbf{p}_0)(\mathbf{p} - \mathbf{p}_0)$ .

We now consider how the angular component of a vector field changes on an infinitesimal circle  $\Gamma$  centered at  $\mathbf{p}_0$ . Given a point  $\mathbf{p} \in \Gamma$ , we have  $\mathbf{p} = \mathbf{p}_0 + \begin{pmatrix} r \cos \theta \\ r \sin \theta \end{pmatrix}$  where  $(r, \theta)$  are the polar coordinates. The local linearization at  $\mathbf{p}_0$  is  $LV(\mathbf{p}) = r \begin{pmatrix} a \cos \theta + b \sin \theta \\ c \cos \theta + d \sin \theta \end{pmatrix}$ . The angular component is

$$\tan^{-1} \left( \frac{c \cos \theta + d \sin \theta}{a \cos \theta + b \sin \theta} \right) \quad (4)$$

which has a derivative

$$\frac{ad - bc}{(a \cos \theta + b \sin \theta)^2 + (c \cos \theta + d \sin \theta)^2} \quad (5)$$

When  $ad - bc \neq 0$ , the sign of the quantity  $ad - bc$  is related to the *Poincaré index* of  $\mathbf{p}_0$ , which is defined in terms of the *winding number* for the *Gauss map*.

Let  $V$  be a continuous planar vector field and  $D_0 \subset \mathbb{R}^2$  be the zero set for  $V$ . The *Gauss map*  $\varepsilon : \mathbb{R}^2 \setminus D_0 \rightarrow S^1$  is defined as  $\varepsilon(x) = \frac{V(x)}{|V(x)|}$ .  $\varepsilon$  is continuous in  $\mathbb{R}^2 \setminus D_0$ . In particular, it introduces a continuous map  $\varepsilon|_{\Gamma}$  on any simple loop  $\Gamma$  that does not contain any singularity. When traveling along  $\Gamma$  in the positive direction once, the image under  $\varepsilon|_{\Gamma}$  necessarily covers the unit circle  $S^1$  an integer number of times counting orientation. This integer is the *winding number* of  $V$  along  $\Gamma$ . The Poincaré index of an isolated singularity  $\mathbf{p}_0$  is the winding number of any simple loop that encloses  $\mathbf{p}_0$  and contains no other singularities either in its interior or on the boundary. Denote this number as  $\kappa(V; \mathbf{p}_0)$ . The Poincaré index is  $+1$  for sources, sinks, centers, and foci. It is  $-1$  for saddles, and  $0$  for regular points.

The *Poincaré-Hopf theorem* links the topology of a vector field to that of the underlying domain in the following way. Let  $M$  be a closed orientable manifold with an Euler characteristic  $\chi(M)$ . Furthermore, let  $V$  be a continuous vector field defined on  $M$  with only isolated singularities  $\mathbf{p}_1, \dots, \mathbf{p}_n$ . Then

$$\sum_{i=1}^n \kappa(V; \mathbf{p}_i) = \chi(M) \quad (6)$$

We now extend the concepts of singularities to  $N$ -RoSy fields where  $N \geq 2$ . Given a planar  $N$ -RoSy field  $S$ , we define  $V_S(\mathbf{p}) = \gamma(S(\mathbf{p}))$  as the *representation vector field* of  $S$ . Then, a point  $\mathbf{p}_0$  is an isolated singularity of  $S$  if and only if it is also an isolated singularity of  $V_S$ . We define the index of a singularity  $\mathbf{p}_0$  with respect to  $S$  as

$$\kappa(S; \mathbf{p}_0) = \frac{\kappa(V_S; \mathbf{p}_0)}{N} \quad (7)$$

A singularity  $\mathbf{p}_0$  is of  $L$ -th order if its index is  $|\frac{L}{N}|$ .  $\mathbf{p}_0$  is *positive*, *negative*, or *regular* if  $\kappa(S; \mathbf{p}_0) > 0$ ,  $\kappa(S; \mathbf{p}_0) < 0$ , or  $\kappa(S; \mathbf{p}_0) = 0$ , respectively. As in the case of vector fields and tensor fields, an  $L$ -th order singularity can be constructed by clustering  $L$  first-order singularities [Scheuermann et al. 1998; Delmarchelle and Hesselink 1994]. Assuming an  $N$ -RoSy field has first-order singularities only,  $N|\chi(M)|$  provides a lower bound on the number of singularities in the field. While more singularities can occur, their signed sum remains constant, i.e.,  $\chi(M)$ .

Figure 2 shows natural symmetries on the Platonic solids. To understand what symmetry is natural in a shape, let us consider the total angle around a vertex of the cube, which is  $\frac{3\pi}{2}$ . In order to admit continuity across such a corner, one must accept a rotation of  $\frac{\pi}{2}$ , which is essentially the case when  $N = 4$ . Similarly, an octahedron naturally admits 3-RoSy's, an icosahedron admits 6-RoSy's, a dodecahedron admits 10-RoSy's, and a tetrahedron admits 2-RoSy's (tensors). In all these cases, there are  $K$  first-order positive singularities where  $K$  is the number of vertices in the shape. Furthermore, the total signed index sum is 2, which is the Euler characteristic of a genus-zero surface. Let  $\beta$  be the *angle of deficit* of a vertex, which equals  $2\pi$  minus the total angle around the vertex.  $\beta \neq 0$  implies that the neighborhood of the vertex is likely to admit an  $N = \frac{2\pi}{|\beta|}$  symmetry. When  $\beta > 0$ , the vertex is a positive singularity, and when  $\beta < 0$ , the vertex is a negative singularity. Next, we discuss the separatrices in an  $N$ -RoSy field.

## 4.2 Separatrices

A *separatrix* in a vector field is a trajectory that passes through a saddle. The *topology* of a vector field on a two-dimensional surface consists of singularities and separatrices. Extending the definition of *separatrices* to  $N$ -RoSy fields when  $N \geq 2$  is more difficult because separatrices can emanate from singularities with a positive index. To address this, Delmarcelle and Hesselink [1994] define separatrices for a tensor field (2-RoSy) as the boundaries of a *hyperbolic sector*, which is a region in the vicinity of a singularity inside which trajectories sweep pass the singularity. As an example, there are four hyperbolic sectors for every saddle.

We adopt this approach and define separatrices of an  $N$ -RoSy field  $S$  as the boundary of a hyperbolic sector for a singularity. Figure 5 (a-d) show the four hyperbolic sectors for a positively-indexed singularity in a 3-RoSy field, and (e) their composition. The red lines are *incoming separatrices* and the green lines are *outgoing separatrices*. In (f) we show the separatrices of a negatively-index singularity in a 4-RoSy field. When  $N$  is even, separatrices do not have directions. Notice when  $N \geq 3$ , hyperbolic sectors can overlap, which is a reflection of the fact that there are  $N$  member vectors. When  $N$  is even, there are  $\frac{N}{2}$  streamlines passing through every non-singular point. When  $N$  is odd, there are  $N$  such streamlines.

To extract separatrices, we make use of the following observation: a separatrix approaches a singularity in a radial direction. In other words, given an isolated singularity  $\mathbf{p}_0$ , we consider its local linearization  $DS = \begin{pmatrix} a & b \\ c & d \end{pmatrix}$ , which is defined in terms of the linearization of the representation vector field. On an infinitesimal circle centered at  $\mathbf{p}_0$ , we consider directions  $\mathbf{v} = \mathbf{p} - \mathbf{p}_0$  such that  $\mathbf{v}$  is also a member vector at  $\mathbf{p}$ . Let  $\phi$  be the angular coordinate of one of the member vectors. The aforementioned statement is equivalent to finding directions  $\mathbf{v} = \begin{pmatrix} \cos \theta \\ \sin \theta \end{pmatrix}$  such that

$$N\theta \equiv N\phi \pmod{2\pi} \quad (8)$$

which can be used to find a separatrix that passes through the singularity. Note that this is consistent with the definitions of separatrices in vector fields [Tricoche 2002] and tensor fields [Delmarcelle and Hesselink 1994]. The condition can be rewritten as

$$\frac{\sin N\theta}{\cos N\theta} = \frac{c \cos \theta + d \sin \theta}{a \cos \theta + b \sin \theta} \quad (9)$$

Recall that

$$\cos N\theta = \sum_{i=0}^N \cos \frac{i\pi}{2} \binom{N}{i} \cos^{N-i} \theta \sin^i \theta \quad (10)$$

$$\sin N\theta = \sum_{i=0}^N \sin \frac{i\pi}{2} \binom{N}{i} \cos^{N-i} \theta \sin^i \theta \quad (11)$$

Consequently, solving Equation 9 amounts to finding the roots of an  $(N+1)$ -th order polynomial.

A first-order negative singularity has  $N+1$  separatrices while a first-order positive singularity has at most  $N+1$  separatrices. Note that the above definition extracts all the separatrices in an  $N$ -RoSy field  $S$  only when  $N$  is even. In case  $N$  is odd, the solutions to Equation 9 correspond to the outgoing separatrices only. To capture the incoming separatrices, we need to compute the solutions to

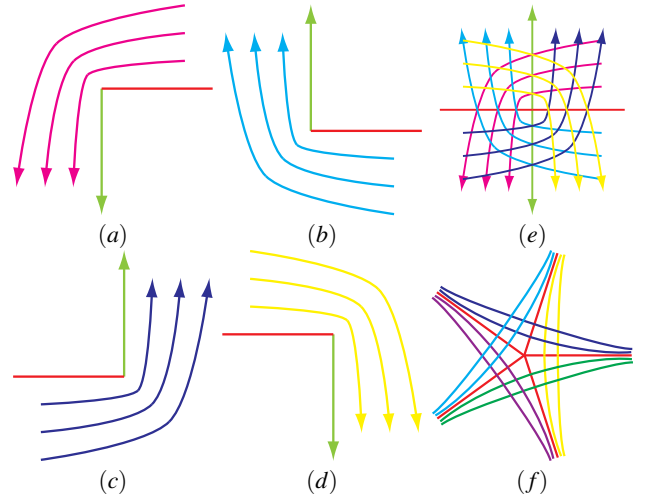


Figure 5: The separatrices of an  $N$ -RoSy field are the boundaries of the hyperbolic sectors in the vicinity of a singularity. In (a)-(d), we show the four hyperbolic sectors for a positive singularity of a 3-RoSy field. These sectors overlap and each of them has an incoming separatrix (red line) and an outgoing separatrix (green line). Together, they describe the topology of the field near the singularity (e). In (f), we show the separatrices for a negative singularity in a 4-RoSy field. Notice that separatrices do not have directions when  $N$  is even.

$$N\theta \equiv N\phi + \pi \pmod{2\pi} \quad (12)$$

which is equivalent to computing the separatrices of  $-S$ . Next, we describe how we represent an  $N$ -RoSy field on a triangular mesh surface and how to extract the topological features in the discrete setting.

## 4.3 Discrete Representation

On a triangular mesh, we use a vertex-based representation for an  $N$ -RoSy field  $S$ . In such a setting, the values of  $S$  are defined at the vertices and interpolations are used to obtain values on edges and inside triangles. Note that in practice we use the representation vector field  $V_S$  instead of  $S$  itself.

When the triangular mesh represents a planar domain, we use the popular piecewise linear interpolation scheme of vector fields [Tricoche 2002]. Basically, inside every triangle the representation vector field  $V_S$  is *linear* and therefore can be expressed as  $\begin{pmatrix} ax+by+e \\ cx+dy+f \end{pmatrix}$  under the global coordinate systems. Here,  $\begin{pmatrix} a & b \\ c & d \end{pmatrix}$  is the Jacobian of the representation vector field, and it is constant inside every triangle. This representation supports efficient singularity and separatrix extraction. We perform the following steps in computing the topology of an  $N$ -RoSy field.

1. We locate the singularities of the representation vector field using the method in [Tricoche 2002] and compute the linearization, which is constant for each triangle.
2. We extract separatrix directions by solving Equation 9 for every singularity.
3. For each separatrix direction  $w$ , we perform streamline tracing

from a point sufficiently close to the singularity in the direction of  $w$ .

On meshes that represent curved surfaces, the above piecewise linear scheme no longer produces continuous  $N$ -RoSy fields. We refer the readers to [Zhang et al. 2006] for an example when  $N = 1$ . Furthermore, a curved surface in general lacks a global parameterization and consistent local frames. To overcome these problems, Zhang et al. [2006] develop a non-linear interpolation scheme that produces continuous vectors fields and supports efficient singularity and separatrix extraction. Their scheme is based on the ideas of *geodesic polar maps* and *parallel transport* from differential geometry. Extending this scheme to  $N$ -RoSy fields is straightforward, and it has been done when  $N = 2$  [Zhang et al. 2007]. Recently, Wang et al. [2006] have proposed another scheme based on edge subdivision and discrete differential forms. Adapting their scheme to  $N$ -RoSy fields is also promising.

## 5 Design of $N$ -RoSy Fields

In this section, we describe our design system for  $N$ -RoSy fields on 3D surfaces. In our approach, the user can create a field either from scratch or by modifying an existing field, such as the curvature tensor. Our system allows a user to add features to the field, to remove unwanted singularities, and to relocate singularities to more natural locations. These functionalities can be used in pen-and-ink sketching to reduce visual artifacts caused by singularities (Section 6.1) and in geometry remeshing to maintain geometry details (Section 6.2).

Our design system employs a two-stage pipeline: initialization and editing. In the first stage, the user quickly creates or modifies an  $N$ -RoSy field through a set of constraints called *design elements*. Design elements can be in the forms of desired orientations or singularities at a given point. The field obtained this way often contains unwanted or misplaced singularities, which can be handled in the second stage through editing operations such as singularity pair cancellation and movement. This pipeline is consistent with the design systems for vector fields [Zhang et al. 2006] and tensor fields [Zhang et al. 2007] when  $N = 1$  and  $N = 2$ , respectively. Given the intrinsic connection between an  $N$ -RoSy and its representation vector, our design system can be adapted from a vector field design system such as [Zhang et al. 2006]. Next, we describe our implementations for both stages.

### 5.1 Initialization

There have been a number of techniques for creating a vector field on a 3D surface, such as blending basis fields on surfaces [Zhang et al. 2006] or in 3D [van Wijk 2003], relaxation [Turk 2001; Wei and Levoy 2001], and propagation [Praun et al. 2000]. These approaches provide tradeoffs among a number of factors such as controllability, interactivity, and ease of use. For planar domains, the idea of using basis fields is highly desirable due to its simplicity and intuitiveness [van Wijk 2002]. We employ this approach to create an  $N$ -RoSy field  $S$  in the plane by creating its representation vector field  $V_S$ . Basically, given a set of constraints  $C = \{c_1, \dots, c_k\}$ , we define  $V_S = \sum_{i=1}^k V_{S_i}$  where

$$V_{S_i}(\rho, \theta) = e^{-d\rho^2} \begin{pmatrix} \cos N(\frac{L\theta}{N} + \theta_0) \\ \sin N(\frac{L\theta}{N} + \theta_0) \end{pmatrix} \quad (13)$$

In the above equation,  $(\rho, \theta)$  are the polar coordinates of a point  $(x, y)$  with the center of  $c_i$  being the origin.  $\theta_0$  is the phase shift constant that can turn a source into a sink or a center when  $N = 1$ .  $L$  is the *order* of the design element. When  $L = 0$ , Equation 13 leads

to a field of a constant direction. When  $L \neq 0$ , the design element is either a *positive* or *negative*  $L$ -th order element. Finally,  $d$  is a constant that is used to describe the falloff speed in the strength of  $V_{S_i}$ . Such a falloff function enables fast blending of basis fields so that a user-desired pattern is not affected by other basis fields [van Wijk 2002].

While our system can be used to generate singularities of arbitrary orders, we are primarily interested in the cases when  $L = 0$  or  $L = \pm 1$  since an  $L$ -th order element can be simulated by combining  $L$  first-order elements.

On surfaces, the idea of blending basis vector fields encounters a serious difficulty, i.e., Equation 13 requires a global parameterization, which is often unavailable for a 3D surface. Zhang et al. [2006] address this problem by computing a global parameterization with respect to each design element. However, this approach is rather expensive. Van Wijk [2003] creates volume basis vector fields before projecting them onto the tangent planes. While this approach is fast, it is difficult to achieve local patterns such as sources, sinks, and saddles due to surface curvature.

Relaxation techniques such as [Turk 2001; Wei and Levoy 2001] provide a nice balance between controllability and computational cost. In this approach, vector values are defined at a (small) number of vertices. Then, values elsewhere are obtained by solving a Laplace equation on each of the three components of the vector field with the specified vector values being the boundary conditions. While being fast and intuitive, two issues must be addressed before we can use such an approach to create  $N$ -RoSy fields on surfaces. First, how do we automatically generate vector values so that the resulting  $N$ -RoSy field contains the desired singularities. Second, directly performing relaxation on the representation vector field  $V_S$  is likely to produce undesired results as  $V_S$  depends on the local frame. Yet, without a global parameterization, local frames at the vertices are typically uncorrelated.

The first issue can be resolved relatively easily. Given a design element whose  $L = -1, 0, 1$ , we can compute the  $N$ -RoSy values at the three vertices of the triangle containing the design element. When  $|L| > 1$ , the support of the element is larger than one triangle. In practice, we find it sufficient to only specify zeroth- and first-order design elements as an  $L$ -th order element can be created by designing  $L$  first-order elements.

The second issue is more challenging, and it is related to the concept of parallel transport from differential geometry. Consider two points  $\mathbf{p}$  and  $\mathbf{q}$  on the surface  $M$  and a geodesic  $\Gamma: [0, 1] \rightarrow M$  such that  $\Gamma(0) = \mathbf{p}$  and  $\Gamma(1) = \mathbf{q}$ . Given two vectors  $v_{\mathbf{p}}$  and  $v_{\mathbf{q}}$  that are defined at  $\mathbf{p}$  and  $\mathbf{q}$  respectively,  $v_{\mathbf{p}}$  is said to be equivalent to  $v_{\mathbf{q}}$  with respect to  $\Gamma$  if the angle between  $v_{\mathbf{p}}$  and  $\Gamma'(\mathbf{p})$  is equal to the angle between  $v_{\mathbf{q}}$  and  $\Gamma'(\mathbf{q})$ . Recall that the shortest geodesic between the two incident vertices is the edge connecting them. This allows us to set up the Laplace equation  $\nabla^2 V = 0$  and its discrete form on a mesh surface,

$$w_i = \sum_{j \in J} \omega_{ij} T_{ij}(w_j) \quad (14)$$

where  $w_i$  is the representation vector value at vertex  $v_i$ ,  $\omega_{ij}$  is the mean value coordinate [Floater 2003] and  $T_{ij}$  is the transport function from the tangent plane at vertex  $v_j$  to vertex  $v_i$ . Let  $\begin{pmatrix} F_i \\ G_i \end{pmatrix}$  be the coordinates of  $w_i$  under the local frame at vertex  $v_i$ . Equation 14 has the following more explicit form:

$$\begin{pmatrix} F_i \\ G_i \end{pmatrix} = \sum_{j \in J} \omega_{ij} \begin{pmatrix} \cos N\Delta\theta_{ij} & -\sin N\Delta\theta_{ij} \\ \sin N\Delta\theta_{ij} & \cos N\Delta\theta_{ij} \end{pmatrix} \begin{pmatrix} F_j \\ G_j \end{pmatrix} \quad (15)$$

where  $\Delta\theta_{ij}$  is the difference between the angle from the  $X$ -axis to the geodesic at  $\mathbf{q}$  and that from the  $X$ -axis to the geodesic at  $\mathbf{p}$ .

Equation 15 is a sparse linear system that can be solved efficiently by a bi-conjugate gradient solver.

There have been a number of other relaxation methods for smoothing a 4-RoSy field that are similar to our formulation in spirit. Hertzmann and Zorin [2000] define a non-linear functional. While high-quality, it is more time-consuming than linear optimization approaches. Ray et al. [2006a] set up a linear system by performing smoothing on member vectors. As discussed in Section 3, smoothing (adding) member vectors may lead to incoherent results.

Note that none of the aforementioned techniques including relaxation provide explicit control over the number and location of the singularities in the field. Consequently, unwanted or misplaced singularities can occur. We address this issue through topological editing operations such as singularity pair cancellation and movement, to be described next.

## 5.2 Editing

Topological control over an  $N$ -RoSy field requires the ability to perform local modification to the field near a singularity. Our system offers two topological editing operations: *singularity pair cancellation* and *singularity movement*. Singularity pair cancellation allows a first-order positive singularity to be cancelled with a nearby first-order negative singularity. Note that a singularity cannot be removed by itself due to the topological constraints imposed by the surface. Singularity movement allows a singularity to be moved to a more desirable location. Given the vector-based representation of an  $N$ -RoSy field, we perform both operations on its representation vector field, which allows us to reuse corresponding vector field editing algorithms such as [Zhang et al. 2006].

In their framework, singularity pair cancellation and movement operations are implemented in a unified fashion that is based on Conley index theory from dynamical systems [Mischaikow and Mrozek 2002]. According to this theory, to cancel a singularity pair in a vector field that have opposite Poincaré indices, one can systematically find a region that encloses the singularity pair without covering any other singularities. By construction, this region will have a *trivial* Conley index, which means that it is possible to alter the flow inside the region such that no singularity exists after the modification. Singularity movement is performed similarly. Zhang et al. [2006] provide practical algorithms to compute the region and perform vector-valued Laplacian smoothing in order to modify the flow inside. We refer the readers to [Mischaikow and Mrozek 2002] for details on Conley index theory and to [Zhang et al. 2006] for the implementation details on topological editing on vector fields. Figure 6 illustrates topological editing operations on a 4-RoSy field that contains two positive singularities and one negative singularity (left). First, the negative singularity is cancelled with a positive singularity (middle). Next, the remaining singularity is moved (right). The actual pair cancellation and movement operations are conducted on the representation vector fields.

Performing singularity pair cancellation and movement on surfaces requires the ability to conduct Laplacian smoothing on the representational vector field inside a region. To avoid the use of surface parameterization that is computationally expensive, we reuse the idea of parallel transport discussed in Section 5.1, which allows relaxation to be carried out on surfaces.

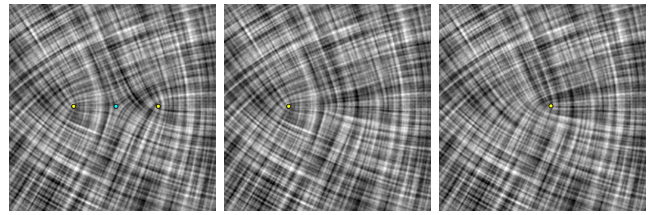


Figure 6: This figure illustrates the topological editing operations of our system. The fields shown in the images are: a 4-RoSy field with three singularities (left), after singularity pair cancellation (middle), and after singularity movement (right). The actual editing was performed on the representation vector fields, which allows us to reuse corresponding vector field editing operations.

## 6 Applications

We have applied our design system to pen-and-ink sketching and quad-dominant remeshing.

### 6.1 Pen-and-ink Sketching of Surfaces

Pen-and-ink sketching of surfaces is a non-photorealistic style of shape visualization. The efficiency of the visualization as well as the artistic appearance depend on a number of factors, one of which is the direction of hatches. Girshick et al. [2000] show that 3D shapes are best illustrated if hatches follow principle curvature directions. However, curvature estimation on discrete surfaces is a challenging problem. While there have been several algorithms that are theoretically sound and produce high-quality results [Hertzmann and Zorin 2000; Meyer et al. 2002; Cohen-Steiner and Morvan 2003; Rusinkiewicz 2004], most of them still rely on smoothing to reduce the noise in the curvature estimate. Consequently, these methods do not provide control over the singularities in the field. Hertzmann and Zorin [2000] propose the concept of cross fields, which are 4-RoSy fields obtained from the curvature tensor (a 2-RoSy field) by removing the distinction between the major and minor principle directions. They demonstrate that smoothing on the cross field tends to produce more natural hatch directions than smoothing directly on the curvature tensor. They also point out the need to control the number and location of the singularities in the field. Zhang et al. [2007] address this issue by providing singularity pair cancellation and movement operations on the curvature tensor field. However, their technique cannot handle a 4-RoSy field.

In this paper, we follow Hertzmann and Zorin [2000] by treating hatch directions as a 4-RoSy field and use topological editing operations to control the number and location of the singularities. Figure 7 illustrates the utility of topological editing operations with the Bimba model. The original 4-RoSy field (left) was obtained from the curvature tensor, which we computed using the algorithm of Meyer et al. [2002]. This field contains three singularities on the visible side of the face, which cause visual artifacts in the result. Two of them (on the lower side of the face near the neck) were removed through singularity pair cancellation (middle), and the third one (near the corner of the right eye) was moved within the high-light region (right).

Figure 1 provides the following comparisons with the Venus model: 2-RoSy (a) versus 4-RoSy (b), and topological editing (c) versus global smoothing (d). Representing the curvature tensor as a 4-RoSy field leads to smoother results. Notice the visual artifacts caused by the singularities on the chest in (a). The hatch directions in those regions are more natural with 4-RoSy's (b). In (c) and (d), we compare topological editing and global smoothing that can both

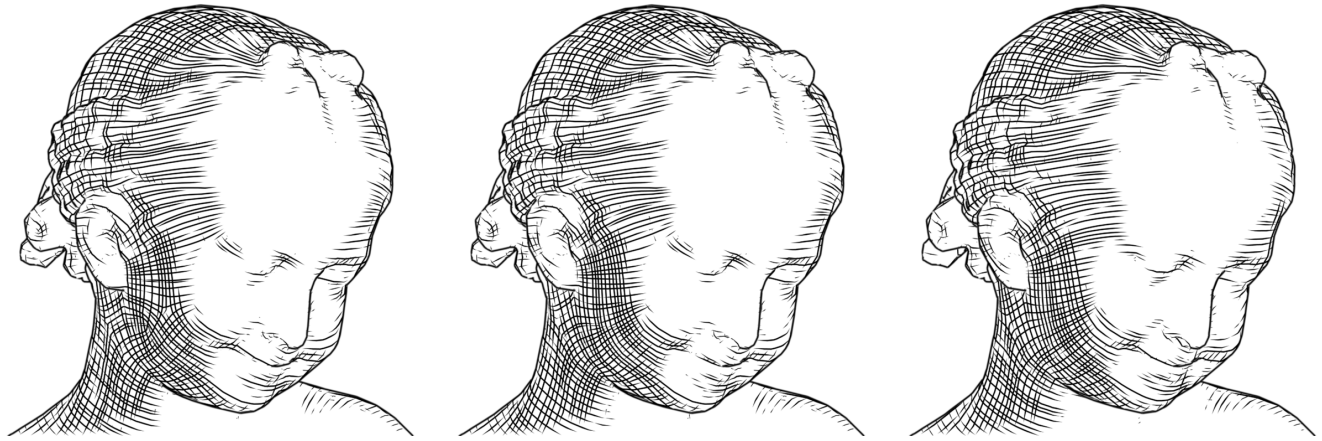


Figure 7: Topological editing operations were applied to pen-and-ink sketching of the Bimba model in order to remove visual artifacts caused by undesirable singularities. The original 4-RoSy field (left) contains a number of such singularities on the visible side of the face (left). Two of them (on the lower side of the face near the neck) were removed through singularity pair cancellation (middle). Next, a singularity near the corner of the right eye was moved to reduce the amount of discontinuity in the hatching directions near the eye.

be used to further reduce the visual artifacts caused by unwanted singularities. Compare these images to (b) near the chest and under the armpit. Furthermore, topological editing operations provide local control that is lacking in global smoothing. Notice that excessive global smoothing can lead to significant deviations in the hatch directions. Compare (b) and (d) around the neck and on the chest. Topological editing operations, on the other hand, preserve curvature directions in regions where topological editing was not performed. See the same regions in (c).

## 6.2 Quad-Dominant Remeshing

The problem of quad-dominant remeshing, i.e., constructing a quad-dominant mesh from an input mesh, has been a well-studied problem in computer graphics. The key observation is that a nice quad-mesh can be generated if the orientations of the mesh elements follow the principle curvature directions [Alliez et al. 2003]. This observation has led to a number of efficient remeshing algorithms that are based on streamline tracing [Alliez et al. 2003; Marinov and Kobbelt 2004; Dong et al. 2005]. Ray et al. [2006a] note that better meshes can be generated if the elements are guided by a 4-RoSy field. They also develop an energy functional that can be used to generate a periodic global parameterization and to perform quad-based remeshing. The connection between quad-dominant remeshing and 4-RoSy fields has also inspired Tong et al. [2006] to generate quad meshes by letting the user design a *singularity graph* that resembles the behavior of the topological skeleton of a 4-RoSy field. On the other hand, Dong et al. [2006] perform quad-remeshing using spectral analysis, which produces quad meshes that in general do not align with the curvature directions.

We apply our design system to a 4-RoSy field that is obtained from principle curvature directions by not distinguishing between the major and minor directions. Our method is based on streamline tracing. In contrast to most existing approaches, we first trace all the separatrices for a certain distance. This allows singularities to be the vertices in the new mesh and that the nearby regions consist of nice quad elements (Figure 8). Notice that this would not have been possible without the analysis of  $N$ -RoSy fields. In addition, 4-RoSy field design enhances the chance of obtaining a better mesh by removing noise and placing singularities in natural locations. Figure 8 illustrates this with two examples fields, both were obtained by editing a 4-RoSy field corresponding to the curvature

tensor. The top field corresponds to a sequence of global smoothing, which tends to lose sharp features in the model and no longer follows the principle curvature directions. The bottom field, on the other hand, was obtained through a sequence of singularity editing operations that allow singularities to be edited in an isolated fashion, thus maintain sharp features and natural singularities.

We wish to emphasize that the focus of our work is on the analysis and design of  $N$ -RoSy fields. While we have employed a streamline-based remeshing approach [Alliez et al. 2003] to demonstrate the capabilities of our system, fields designed using our system can potentially be input to other and more recent remeshing techniques such as [Ray et al. 2006a].

## 7 Conclusion

In this paper, we have developed a design system for  $N$ -RoSy fields on surfaces with explicit control over the number and location of singularities in the fields. We demonstrate the effectiveness of our system with applications in non-photorealistic rendering and quad-dominant remeshing.

As part of our system, we describe a mathematically sound representation for  $N$ -RoSy's that is based on higher-order symmetric tensors. This link allows us to define algebraic operations as well as analytic characteristics such as singularities, differentiability, and continuity. Furthermore, we present a compact vector-based representation of  $N$ -RoSy fields on mesh surfaces that makes it possible to perform field smoothing using linear systems.

We also provide topological analysis of  $N$ -RoSy fields and efficient algorithms with which singularities and separatrices can be identified.

In the future, we plan to investigate the use of 6-RoSy field design to obtain optimal triangulations from an input mesh. Figure 9 demonstrates this potential with a user-guided 6-RoSy field on the dragon. Notice that the streamlines according to field, while not aligned perfectly, intersect at angles that are multiples of  $\frac{\pi}{6}$ . Adaptation of quadrangulation methods such as [Ray et al. 2006a; Tong et al. 2006] has the potential of generating high-quality triangular meshes.

In many applications, multiple, coexisting symmetries of differ-

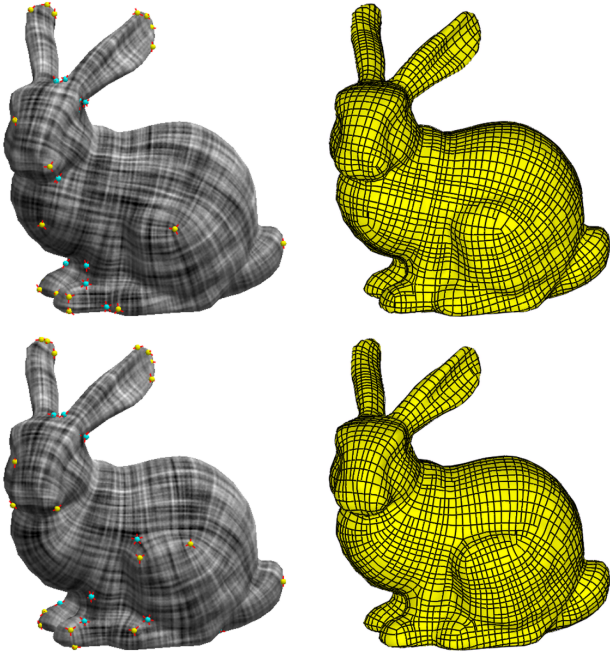


Figure 8: 4-RoSy field design was applied to quad-dominant remeshing. The field in the top was obtained by performing smoothing on a 4-RoSy field derived from the curvature tensor, while the field in the bottom was obtained by performing a sequence of topological editing operations on the same tensor field. Notice that while both fields are smooth, the field in the bottom contains singularities that situate in natural locations such as near the leg. In contrast, the field in the top is overly smooth and does not follow the curvature directions in many parts of the model.

ent  $N$ 's are of interest, such as pen-and-ink sketching and texture synthesis. We plan to investigate a mathematical framework with which such objects can be analyzed and designed.

## Appendix: $N$ -RoSy's and $N$ -th Order Tensors

In this appendix, we point out the link between  $N$ -RoSy's and  $N$ -th order covariant symmetric tensors, which justifies the way in which the components of a representation vector transform under a change of basis (Section 3).

Recall that when  $N = 1$  and 2, an  $N$ -RoSy can be modeled as a vector or a symmetric traceless matrix [Zhang et al. 2007], respectively. When  $N \geq 3$ , we turn to  $N$ -th order tensors and define an injective map  $\alpha$  from the set of two-dimensional  $N$ -RoSy's into the set of two-dimensional  $N$ -th order symmetric tensors.  $\alpha$  allows algebraic operations on  $N$ -RoSy's to be defined in terms of corresponding operations on  $N$ -th order tensors. Before describing  $\alpha$ , we briefly review relevant facts about  $N$ -th order tensors. Given an orthonormal basis for  $\mathbb{R}^2$ , an  $N$ -th order covariant *tensor*  $t = t_{i_1 \dots i_N}$  ( $1 \leq i_1, \dots, i_N \leq 2$ ) is a multi-linear form

$$t(w_1, \dots, w_N) = t_{i_1 \dots i_N} w_1^{i_1} \dots w_N^{i_N} \quad (16)$$

where  $w_j$ 's ( $1 \leq j \leq N$ ) are two-dimensional vectors and  $w_k^{i_k}$  refers to the  $i_k$ -th component of  $w_k$ . Here we are using the *Einstein convention* in which the summation signs are omitted.  $t$  is *symmetric* if  $t_{i_1 \dots i_N} = t_{i_{p(1)} \dots i_{p(N)}}$  for any permutation  $p$  over the set  $\{1, \dots, N\}$ .

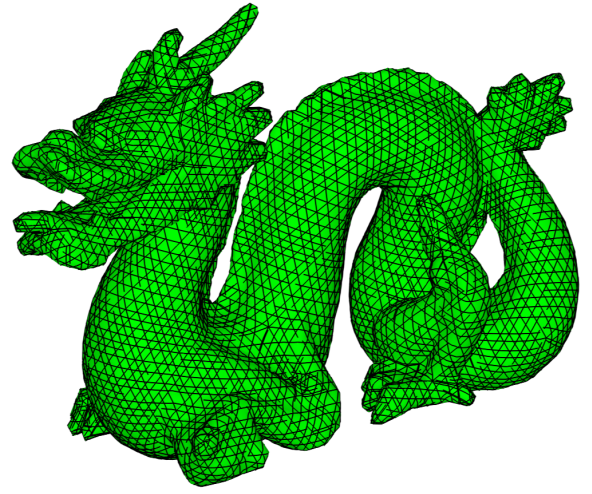


Figure 9: A 6-RoSy field designed using our system. Notice that the network of streamlines resembles a highly regular triangulation.

In the remainder of the discussion we will only focus on covariant and symmetric tensors and therefore omit the words *symmetric* and *covariant* for convenience.

Given an  $N$ -RoSy

$$s = \left\{ R \begin{pmatrix} \cos(\theta + \frac{2k\pi}{N}) \\ \sin(\theta + \frac{2k\pi}{N}) \end{pmatrix} \mid 0 \leq k \leq N-1 \right\} \quad (17)$$

we consider the following  $N$ -th order tensor

$$t_{i_1 \dots i_N} = \begin{cases} R \cos(N\theta) & \text{if } i_1 + i_2 + \dots + i_N \equiv 0 \pmod{4} \\ R \sin(N\theta) & \text{if } i_1 + i_2 + \dots + i_N \equiv 1 \pmod{4} \\ -R \cos(N\theta) & \text{if } i_1 + i_2 + \dots + i_N \equiv 2 \pmod{4} \\ -R \sin(N\theta) & \text{if } i_1 + i_2 + \dots + i_N \equiv 3 \pmod{4} \end{cases} \quad (18)$$

Given a vector  $w = \begin{pmatrix} \cos \phi \\ \sin \phi \end{pmatrix}$ , it is straightforward to verify that  $t(w, \dots, w) = R \cos N(\theta - \phi)$ . Furthermore, it can be shown that  $t$  is the only tensor that has this property.  $t(w, \dots, w)$  achieves its maximum on the unit circle  $S^1$  when  $\theta - \phi \equiv 0 \pmod{\frac{2\pi}{N}}$ . There are  $N$  such vectors, which are exactly the member vectors of  $s$ . This allows us to map  $s$  to  $t = \alpha(s)$  as defined in Equation 18. When  $N = 1$ ,  $s$  is a vector and  $t = s$  is also a vector. When  $N = 2$ ,  $t$  is the traceless symmetric matrix whose major eigenvalue is  $R$  and major eigenvectors are given by the member vectors of  $s$ .

Notice that tensors defined in Equation 18 form a two-dimensional linear subspace of the set of  $N$ -th order tensors, which leads to the following construction of a bijective map  $\beta$  from the subspace to a two-dimensional vector space such that

$$\beta(t_{i_1 \dots i_N}) = \begin{pmatrix} t_{00 \dots 0} \\ t_{10 \dots 0} \end{pmatrix} = \begin{pmatrix} R \cos N\theta \\ R \sin N\theta \end{pmatrix} \quad (19)$$

The composite map  $\gamma = \beta \circ \alpha$  has been used to map an  $N$ -RoSy to its representation vector as described in Section 3. As a compact representation of an  $N$ -th order tensor, the components of a representation vector transform differently than a vector under a change of basis.

## Acknowledgements

We would like to thank the following people and groups for the 3D models they provided: Mark Levoy and the Stanford Graphics Group, Cyberware, and the AIM@SHAPE Shape Repository. The discussions with Greg Turk have been valuable. We are also grateful for the help of Patrick Neill and Guoning Chen in preparing the video production. Finally, we wish to thank our reviewers for their excellent comments and suggestions. This work is funded by NSF grant CCF-0546881.

## References

- ALLIEZ, P., COHEN-STEINER, D., DEVILLERS, O., LÉVY, B., AND DESBRUN, M. 2003. Anisotropic polygonal remeshing. *ACM Transactions on Graphics (SIGGRAPH 2003)* 22, 3 (July), 485–493.
- CHEN, G., MISCHAIKOW, K., LARAMEE, R. S., PILARCZYK, P., AND ZHANG, E. 2007. Vector field editing and periodic orbit extraction using morse decomposition. *IEEE Transactions on Visualization and Computer Graphics* 13, 4, 769–785.
- COHEN-STEINER, D., AND MORVAN, J. 2003. Restricted delaunay triangulations and normal cycle. In *19th Annual ACM Symposium Computational Geometry*.
- DELMARCELLE, T., AND HESSELINK, L. 1994. The topology of symmetric, second-order tensor fields. *IEEE Computer Graphics and Applications*, 140–147.
- DONG, S., KIRCHER, S., AND GARLAND, M. 2005. Harmonic functions for quadrilateral remeshing of arbitrary manifolds. *Computer Aided Geometry Design*. (to appear in upcoming Special Issue on Geometry Processing).
- DONG, S., BREMER, P.-T., GARLAND, M., PASCUCCI, V., AND HART, J. C. 2006. Spectral surface quadrangulation. *ACM Trans. Graph.* 25, 3, 1057–1066.
- FLOATER, M. S. 2003. Mean value coordinates. *CAGD*, 20, 19–27.
- GIRSHICK, A., INTERRANTE, V., HAKER, S., AND LEMOINE, T. 2000. Line direction matters: an argument for the use of principal directions in 3D line drawings. *Proceedings of NPAR*, 43–52.
- HELMAN, J. L., AND HESSELINK, L. 1991. Visualizing vector field topology in fluid flows. *IEEE Computer Graphics and Applications* 11 (May), 36–46.
- HERTZMANN, A., AND ZORIN, D. 2000. Illustrating smooth surfaces. *Computer Graphics Proceedings, Annual Conference Series (SIGGRAPH 2000)* (Aug.), 517–526.
- MARINOV, M., AND KOBBELT, L. 2004. Direct anisotropic quad-dominant remeshing. *Computer Graphics and Applications, 12th Pacific Conference on (PG'04)*, 207–216.
- MEYER, M., DESBRUN, M., SCHRÖDER, P., AND BARR, A. H. 2002. Discrete differential-geometry operators for triangulated 2-manifolds. *VisMath*.
- MISCHAIKOW, K., AND MROZEK, M. 2002. Conley index. *Handbook of Dynamic Systems, North-Holland* 2, 393–460.
- PRAUN, E., FINKELSTEIN, A., AND HOPPE, H. 2000. Lapped textures. *Computer Graphics Proceedings, Annual Conference Series (SIGGRAPH 2000)* (Aug.), 465–470.
- RAY, N., LI, W. C., LÉVY, B., SHEFFER, A., AND ALLIEZ, P. 2006. Periodic global parameterization. *ACM Transactions on Graphics* 25, 4, 1460–1485.
- RAY, N., VALLET, B., LI, W.-C., AND LEVY, B. 2006. N-symmetry direction fields on surfaces of arbitrary genus. In *Tech Report*.
- RUSINKIEWICZ, S. 2004. Estimating curvatures and their derivatives on triangle meshes. In *3DPVT '04: Proceedings of the 3D Data Processing, Visualization, and Transmission, 2nd International Symposium on (3DPVT'04)*, 486–493.
- SCHUEERMANN, G., KRGER, H., MENZEL, M., AND ROCKWOOD, A. P. 1998. Visualizing nonlinear vector field topology. *IEEE Transactions on Visualization and Computer Graphics* 4, 2, 109–116.
- STAM, J. 2003. Flows on surfaces of arbitrary topology. *ACM Transactions on Graphics (SIGGRAPH 2003)* 22, 3 (July), 724–731.
- THEISEL, H. 2002. Designing 2d vector fields of arbitrary topology. In *Computer Graphics Forum (Proceedings Eurographics 2002)*, vol. 21, 595–604.
- TONG, Y., LOMBAYDA, S., HIRANI, A., AND DESBRUN, M. 2003. Discrete multiscale vector field decomposition. *ACM Transactions on Graphics (SIGGRAPH 2003)* 22, 3 (July), 445–452.
- TONG, Y., ALLIEZ, P., COHEN-STEINER, D., AND DESBRUN, M. 2006. Designing quadrangulations with discrete harmonic forms. *ACM/Eurographics Symposium on Geometry Processing*, 201–210.
- TRICOCHE, X. 2002. *Vector and Tensor Field Topology Simplification, Tracking, and Visualization*. PhD thesis, Universität Kaiserslautern.
- TURK, G. 2001. Texture synthesis on surfaces. *Computer Graphics Proceedings, Annual Conference Series (SIGGRAPH 2001)*, 347–354.
- VAN WIJK, J. J. 2002. Image based flow visualization. *ACM Transactions on Graphics (SIGGRAPH 2002)* 21, 3 (July), 745–754.
- VAN WIJK, J. J. 2003. Image based flow visualization for curved surfaces. In: *G. Turk, J. van Wijk, R. Moorhead (eds.), Proceedings IEEE Visualization* (Oct.), 123–130.
- WANG, K., WEIWEI, TONG, Y., DESBRUN, M., AND SCHRÖDER, P. 2006. Edge subdivision schemes and the construction of smooth vector fields. *ACM Transactions on Graphics* 25, 3, 1041–1048.
- WEI, L. Y., AND LEVOY, M. 2001. Texture synthesis over arbitrary manifold surfaces. *Computer Graphics Proceedings, Annual Conference Series (SIGGRAPH 2001)*, 355–360.
- YING, L., HERTZMANN, A., BIEMANN, H., AND ZORIN, D. 2001. Texture and shape synthesis on surfaces. *Proc. 12th Eurographics Workshop on Rendering*, 301–312.
- ZHANG, E., MISCHAIKOW, K., AND TURK, G. 2006. Vector field design on surfaces. *ACM Transactions on Graphics* 25, 4, 1294–1326.
- ZHANG, E., HAYS, J., AND TURK, G. 2007. Interactive tensor field design and visualization on surfaces. *IEEE Transactions on Visualization and Computer Graphics* 13, 1, 94–107.